Z. Phys. A – Atomic Nuclei 336, 369–374 (1990)

Zeitschrift für Physik A
Atomic Nuclei


# $Q_\beta$-Measurements of indium, tin and antimony isotopes with masses $A = 128$ and 130

**U. Stöhlker*, A. Blönnigen**, W. Lippert***, and H. Wollnik**

II. Physikalisches Institut der Justus-Liebig Universität Giessen, Federal Republic of Germany

Received December 5, 1989; revised version February 20, 1990

$\beta$-decay energies of neutron rich tin, antimony and tellurium isotopes with mass number $A = 128$ and 130 were measured. The results obtained are discussed within the framework of earlier measurements. Additionally nuclear masses deduced from the experimental $Q_\beta$-values are compared with mass formulae predictions.

**PACS:** 21.10.Dr; 27.60.+j

## 1. Introduction

About two decades ago first systematic studies were performed to experimentally determine total $\beta$-decay energies of tin, antimony and tellurium nuclei in the vicinity of the doubly magic nucleus $^{132}$Sn. All these studies had been performed using plasma type ion sources at OSIRIS and TRISTAN [1–5]. In general mass-values, which can be deduced from $Q_\beta$-values, of nuclei far away from the region of $\beta$-stability are of considerable interest for the understanding of the *r*-process in the nucleosynthesis, for the testing of theoretical mass-formulae and for decay heat calculations. But furthermore, since most of the nuclei investigated here are $\beta$-decaying from different isomeric states which at present are known not to be interconnected by internal transitions, $Q_\beta$-measurements offer the posibility to get information about properties of these states, which especially in the case of $^{130}$In, are of importance for determinations of shell model parameters in this region.

From a study of the cumulative yields and the isomeric ratios performed at OSTIS [6] it became evident, that for indium isotopes in the mass range $123 \leq A \leq 129$ at odd mass numbers high spin states and at even mass numbers low spin states are preferentially fed. At mass $A = 130$ a quantitative expression has not yet been given, but the experimental results obtained indicate, that the relative feeding of the low spin state is even stronger as compared to $^{128}$In where it was determined with 66%. Due to the chemical selectivity of the high temperature ion source, samples of the most neutron-rich isotopes are not disturbed by isobaric contaminants with higher *Z*, known to be much more abundant in the fission of $^{235}$U. Secondly, in both isobaric chains investigated, the strength of different isomers of tin, antimony and tellurium depend through $\beta$-decay relations only on the yields of the corresponding indium isomers, whereas plasma type ion sources approximately reproduce the isomeric yields of these nuclei obtained after thermal neutron induced fission of $^{235}$U. Of course, both experimental procedures offer advantages. But since we applied a production mechanism, known to produce highly pure samples of indium radionuclides, we started a series of $\gamma\gamma$- and $\beta\gamma$-measurements aiming to improve the knowledge about these near-to-closed-shell nuclei, acquired during the past 18 years. Here we report on the results of the $Q_\beta$-measurements.

## 2. Experimental procedures

$Q_\beta$-measurements on indium isotopes and their $\beta$-decay daughters with masses $A = 128$ and 130 were performed at the on-line mass separator OSTIS installed at the high-flux reactor in Grenoble with measuring periodes of 1 and 5 days, respectively. The separator was equipped with a high-temperature ion source [7] providing sources of indium from thermal neutron induced fission of $^{235}$U with a contamination from neighbouring masses of about $10^{-4}$.

Listmode formatted $\beta\gamma$-coincidence matrices were recorded on a PDP-11 based data-acquisition system sampling signals from a high precision Ge(HP)-$\Delta E$-(Gas) $\beta$-telescope [8] correlated in time to events from a 40% Ge(HP) $\gamma$-detector. Both detectors were mounted under

* Part of a doctoral thesis, Universität Giessen
Permanent address: Institut für Atmosphärische Radioaktivität, D-7800 Freiburg, Federal Republic of Germany
** Permanent address: Kinetic Systems International, D-7800 Freiburg, Federal Republic of Germany
*** Permanent address: Institut Laue-Langevin, F-38000 Grenoble, France

an angle of 180 degrees at distances of approximately 3.0 cm and 5.0 cm relative to a fixed mylar tape on which the mass separated indium ions were collected. To reduce the $\gamma$-background competing with the radiation from the decay of about 600(200) ions per second of $^{128}In(^{130}In)$ at the measuring position, the whole detector set-up was shielded with lead.

## 3. Data-evaluation

For the energy calibration of the Ge(HP)-$\beta$-detector we used $\gamma$-sources in the range from 0.5 to 3.3 MeV and for energies up to 9.3 MeV the background radiation from neutron capture of iron and nickel. The energy loss of the electrons in the $\Delta E$-Gas detector system is known to be 21(1.5) keV [8]. This error together with the influence of the detector response (5 keV) [9], the nonlinearity (1 keV) and quantizing uncertainty (2 keV) of the 12 bit-ADC and the calibration error (1.0 keV) result in a systematic error of 10.5 keV. The effects of amplification instabilities and pile-up effects have proven to be negligible.

In a first step the $\beta$-spectrum coincident to the $\gamma$-line of interest was obtained after subtraction of a peak- and a background-window taken from the $\beta\gamma$-coincidence matrix. Since in many cases this procedure does not totally compensate background effects, in a second step a constant or a linear function was subtracted from the spectrum. In a third step the Fermi-Kurie parameter $\sqrt{N/FPW}$ was calculated where $N$ is the electron intensity obtained by unfolding the measured spectrum with the detector response function [9], $P$ and $W$ the relativistic electron momentum and energy, respectively, and $F$ is the Fermi function. In many cases the resulting $\beta$-spectra are rather complex, since they are composed by different branches, that means $\beta$-transitions populating excited levels of higher energy connected to the low lying level by $\gamma$-cascades. In the Kurie presentation these branches are linear in energy, therefore, in the last step a weighted least squares fit to the high energy branch gave the $E_\beta$-value and, by adding the level energy, the total $\beta$-decay energy was obtained. If the linear function obtained in the first fit is subtracted from the data, the procedure can be repeated to determine end point energies of low energy branches. As can be seen from Table 2, this was done in the case of the 1221 keV and 193 keV $\gamma$-transitions. The various fit-ranges are listed in Tables 1 and 2. In a few cases it ended well below the $E_\beta$ value due to background problems mentioned above. The total error for each gate is given as the sum of the fit- and the systematic-error. $Q_\beta$-values are calculated from the different $E_\beta$-values as weighted mean.

**Table 1.** $Q_\beta$-values of $\beta$-spectra coincident with different $\gamma$-gates at mass $A=128$. The level and gate energies are due to the results obtained in [13]

| | Gate [keV] | Level [keV] | Fit-range [keV] | $E_\beta$ [keV] | $Q_\beta$ [keV] |
|---|---|---|---|---|---|
| $^{128}In(3^+)$ | 4297.3 | 4297.3 | 2100–4500 | 4650 | 8950 (120) |
| | 3519.6 | 3519.6 | 3500–5500 | 5440 | 8960 (200) |
| | 537.9 | 2642.2 | 3500–5000 | 6050 | 8690 (450) |
| | 1089.2 | 2258.1 | 4200–6100 | 6200 | 8460 (450) |
| | 2104.2 | 2104.0 | 5800–6600 | 6770 | 8870 (240) |
| | 935.0 | 2104.0 | 5800–6800 | 6880 | 8980 (280) |
| | 1168.7 | 1168.7 | 6500–7400 | 7620 | 8790 (350) |
| $^{128}In(8^-)$ | 1973.9 | 4065.6 | 2400–5100 | 5160 | 9225 (170) |
| | 1867.2 | 3958.7 | 2400–5200 | 5250 | 9210 (130) |
| | 1067.2 | 4242.9 | 2500–5100 | 5120 | 9360 (250) |
| | 1054.8 | 4242.9 | 2400–4900 | 4950 | 9190 (200) |
| | 257.2 | 2378.0 | 4200–6600 | 6750 | 9130 (400) |
| $^{128}Sn\ 0^+$ | 680.5 | 833.4 | 200– 380 | 428 | 1261 (23) |
| | 557.3 | 635.1 | 300– 550 | 627 | 1262 (23) |
| | 482.3 | 635.1 | 300– 600 | 625 | 1260 (20) |
| | 404.4 | 635.1 | 300– 600 | 620 | 1255 (25) |
| $^{128}Sb(5^+)$ | 753.9 | 1811.3 | 1700–2500 | 2590 | 4400 (50) |
| | 742.3 | 1811.3 | 1700–2600 | 2570 | 4380 (50) |
| | 314.0 | 1811.3 | 1600–2400 | 2590 | 4400 (40) |

**Table 2.** $Q_\beta$-values of $\beta$-spectra coincident with different $\gamma$-gates at mass $A=130$. The level and gate energies are due to the results obtained in [13]

| | Gate [keV] | Level [keV] | Fit-range [keV] | $E_\beta$ [keV] | $Q_\beta$ [keV] |
|---|---|---|---|---|---|
| $^{130}In(1^-)$ | 1221.0 | 1221.2 | 7000–8200 | 8530 | 9750 (200) |
| | | 4119.9 | 4500–5500 | 5880 | 10000 (150) |
| | 1905.2 | 4119.9 | 4000–5600 | 5770 | 9890 (150) |
| | 2091.6 | 4119.9 | 2000–5600 | 5630 | 9750 (250) |
| $^{130}In(5^+)$ | 408.1 | 2492.4 | 4300–7300 | 7510 | 10000 (250) |
| | 774.4 | 1995.6 | 5300–7700 | 7700 | 9700 (300) |
| $^{130}In(10^-)$ | 2259.1 | 4205.9 | 4000–5000 | 5960 | 10170 (170) |
| $^{130}Sn\ 0^+$ | 192.5 | 697.1 | 1130–1400 | 1429 | 2126 (56) |
| | | 1042.5 | 840–1140 | 1120 | 2163 (40) |
| | 229.2 | 1042.5 | 750–1100 | 1112 | 2155 (22) |
| | 316.5 | 1042.5 | 900–1100 | 1123 | 2166 (60) |
| | 434.6 | 697.1 | 800–1300 | 1403 | 2100 (30) |
| | 779.9 | 1042.5 | 600–1100 | 1112 | 2155 (18) |
| $^{130}Sn\ 7^-$ | 144.8 | 1043.8 | 2500–2900 | 2990 | 4030 (160) |
| | 311.5 | 1043.8 | 1800–2650 | 2900 | 3940 (110) |
| | 899.0 | 1043.8 | 1800–2900 | 2905 | 3950 (60) |
| $^{130}Sb(5^+)$ | 348.5 | 1981.5 | 2300–2750 | 2780 | 4760 (220) |
| | 369.8 | 2832.8 | 1000–2150 | 2230 | 5060 (100) |
| | 647.7 | 2462.9 | 2100–2500 | 2520 | 4980 (150) |
| | 697.5 | 2330.3 | 2200–2650 | 2720 | 5050 (110) |
| | 749.1 | 2765.1 | 1000–1950 | 2070 | 4840 (150) |
| | 816.5 | 2449.6 | 1700–2450 | 2530 | 4980 (60) |
| | 920.5 | 2735.6 | 1300–2200 | 2210 | 4950 (100) |
| | 942.2 | 2575.1 | 1900–2350 | 2500 | 5070 (320) |
| | 1017.6 | 2832.8 | 1300–2100 | 2120 | 4950 (35) |
| | 1046.5 | 1886.1 | 1900–2900 | 3350 | 5240 (450) |
| | 1102.3 | 2735.6 | 1000–2150 | 2210 | 4945 (55) |
| | 1199.8 | 2832.8 | 1000–2000 | 2120 | 4950 (60) |
| $^{130}Sb(8^-)$ | 303.3 | 2404.2 | 1500–2400 | 2470 | 4870 (400) |
| | 330.8 | 2146.1 | 1800–2650 | 2700 | 4850 (170) |
| | 455.4 | 3536.4 | 900–1400 | 1540 | 5080 (90) |
| | 934.9 | 3080.9 | 1300–1800 | 1820 | 4900 (220) |
| | 1443.8 | 3544.7 | 700–1200 | 1300 | 4850 (200) |

**Table 3.** Summary of experimental $Q_\beta$ values obtained in this work compared with earlier results

| | $Q_\beta$ [keV] | $Q_\beta$ (lit.) [keV] | Ref. |
|---|---|---|---|
| $A=128$ | | | |
| In(8$^-$) | 9230 (90) | 9390 (220) | [3] |
| | | 9330 (30) | [10] |
| In(3$^+$) | 8910 (90) | 9310 (160) | [3] |
| | | 8990 (50) | [10] |
| Sn 0$^+$ | 1260 (15) | 1290 (40) | [2] |
| | | 1270 (30) | [12] |
| Sb(5$^+$) | 4395 (30) | 4390 (40) | [2] |
| $A=130$ | | | |
| In(1$^-$) | 9880 (90) | 9300 (500) | [4] |
| | | 10120 (180) | [5] |
| | | 10170 (50) | [10] |
| In(5$^+$) | 9880 (200) | 10730 (150) | [5] |
| | | 10610 (50) | [10] |
| In(10$^-$) | 10170 (170) | 10320 (90) | [5] |
| | | 10250 (30) | [10] |
| Sn 7$^-$ | 3955 (50) | 4000 (310) | [2] |
| Sn 0$^+$ | 2145 (15) | 2190 (30) | [2] |
| Sb(8$^-$) | 4990 (70) | 5900 (300) | [1] |
| Sb(5$^+$) | 4960 (25) | 5020 (100) | [2] |

## 4. Results on $A=128$

In Table 1 the results of all $\gamma$-gates specific to the $A=128$ nuclei investigated are shown. Table 3 compares these results with the experimental $Q_\beta$-values from literature. In general the agreement is good. The $Q_\beta$-value of $^{128}$Sn reported by Aleklett et al. [3] seems to be overestimated, since the value reported recently by Fogelberg et al. [10] is close to our result. The $Q_\beta$-value of $^{128}$Sn was found to be 1260(15) keV. This result is based on $\beta$-spectra coincident to four $\gamma$-transitions placed according to the decay scheme of [11]. Three transitions originating from the decay of the (5$^+$)-state in $^{128}$Sb were used to determine the $Q_\beta$-value of this nucleus to be 4395(30) keV which is in agreement with the result obtained in [2]. Hindered by the weakness of all transitions following the decay of the (8$^-$)-state we did not attempt to determine the difference between the isomeric- and groundstate of this nucleus which is expected to be less than 20 keV [2].

## 5. Results on $A=130$

All $E_\beta$-values obtained in the present work are compiled in Table 2. In Table 3 the derived $Q_\beta$-values are presented together with previously published results.

### 5.1. $Q_\beta$-value of $^{130}$In

The calculation of $Q_\beta$-values of the (1$^-$)-, (5$^+$)- and (10$^-$)-states of $^{130}$In is based on the evaluation of 3, 2 and 1 $\gamma$-coincident $\beta$-spectra, respectively. In the case of the (1$^-$)-isomer the 1221 keV- and 4120 keV-states, interconnected by strong $\gamma$-transitions are preferentially fed by $\beta$-decay and thus, as can be seen from Fig. 1a, a low- and high-energy component in the $\beta$-spectrum coincident to the 1221 keV-transition was fitted. Analogous to the data presented in [5] Fig. 1b contains $\beta$-spectra coincident to the 1221 keV- and 1905 keV-transitions, assigned to the (1$^-$)-isomer, and the 2259 keV-transition, assigned to the (10$^-$)-isomers, respectively. As can be seen from the lower part of Table 3 experimentally determined $\beta$-decay energies of $^{130}$In differ considerably. Although the error bars of the $\beta$-decay energies obtained in our measurement are larger than those reported by Fogelberg et al. [5] and [10], the comparison between all these investigations shows that the decay energies from the (10$^-$)-states are consistent within the error bars, but the relative energies of the (1$^-$)- and the (5$^+$)-states obtained differ from 0 keV by about 0.8 MeV. Taking into account the results shown in Table 2 one finds, that with the exception of the 1221 keV-transition $E_\beta$-values of the two negative parity isomers are below 6 MeV, whereas both transitions assigned to the (5$^+$)-isomer have $E_\beta$-values above 7.5 MeV. Comparing Fig. 1 with the $\beta$-spectrum coincident to the 1221 keV-transition shown in [5] the difference between the $Q_\beta$-values of the (5$^+$)-isomer obtained by Fogelberg et al. and us can be explained as due to different energy calibrations for electrons with energies above 6 MeV, taking into account that the energy calibration of the detector system has been performed up to an energy of 4 MeV, respectively 9.3 MeV by Fogelberg et al. [5] and us. Nevertheless, this conclusion ignores that Fogelberg et al. base the $Q_\beta$-value of the (5$^+$)-state on three additional $\gamma$-transitions with $E_\beta$-values up to 6.3 MeV. Therefore further experiments have to be performed to get unambiguous information about the energetic distance and the ordering of the three $\beta$-emitting states in $^{130}$In.

### 5.2. $Q_\beta$-value of $^{130}$Sn

Already in one of the first publications on the decay of $^{130}$In [4] it became evident that the 4$^+$-member of the groundstate band of $^{130}$Sn is placed above the 7$^-$-state, which becomes isomeric, since transitions to all lower lying levels (which have spins $I \leqq 2$, $\pi=+$) are strongly forbidden. According to the fact that the 7$^-$-state lies 1947 keV above the ground state of $^{130}$Sn [12] we calculated from our data, that in $^{130}$Sb the (8$^-$)-state is placed 137(52) keV above the (5$^+$)-state and that the $Q_\beta$-value of $^{130}$Sn is thus 2145(15) keV. Concerning the 193 keV-transition, Table 2 contains two entries, which are due to a low-energy and a high-energy branch originating from $\beta$-decay to the 1043 keV- and the 697 keV-states, respectively.

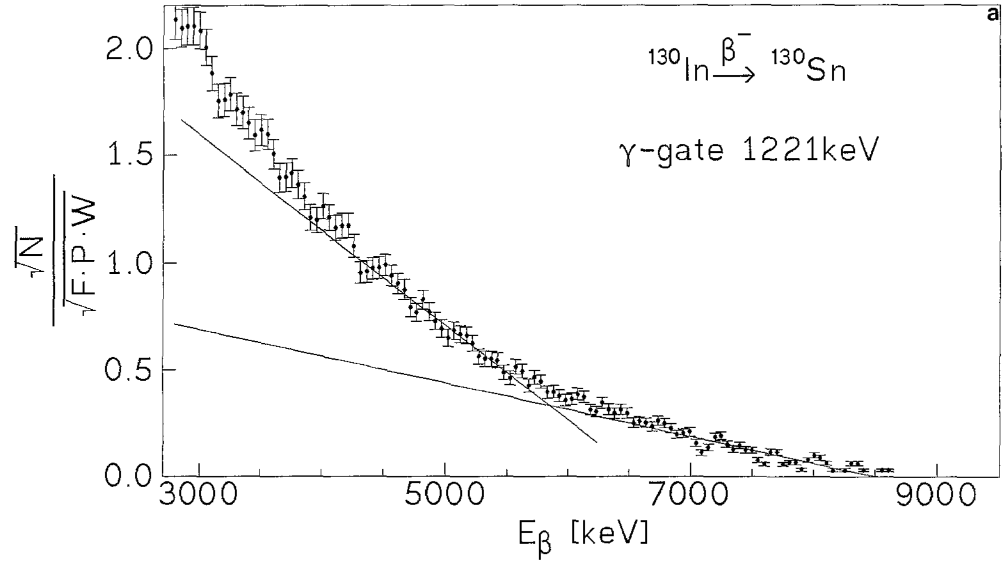


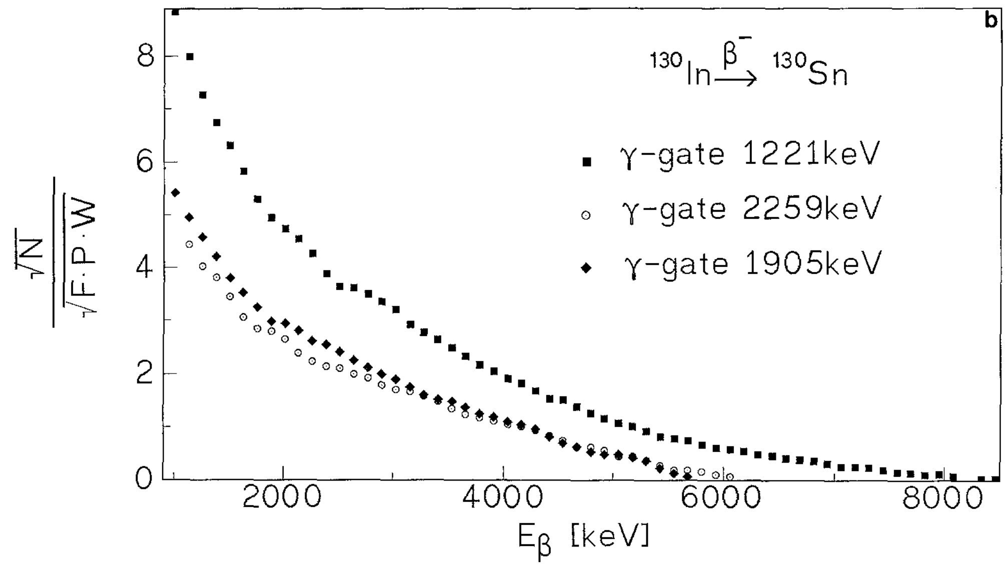


**Fig. 1. a** β-spectrum coincident to the 1221 keV γ-transition from the decay of $^{130}$In **b** β-spectra coincident to the 1221 keV, 1905 keV and 2259 keV γ-transitions from the decay of $^{130}$In

### *5.3. $Q_\beta$-value of $^{130}$Sb*

To confirm this result we additionally calculated the energy of both states relative to the ground state of the even-even nucleus $^{130}$Te. As can be seen from Fig. 2 we placed the $(5^+)$-isomeric state in $^{130}$Sb 4960(25) keV above the ground state of $^{130}$Te which is in good agreement with the value of 5020(100) keV reported by [2]. From 5 γ-coincident β-spectra we obtained a decay energy from the $(8^-)$-state of 4990(70) keV yielding a difference between the isomeric and the ground state of 30(75) keV which is consistent with the value of 137(52) keV mentioned above. The strong 732 keV transition was not taken into account since from γγ-coincidence data this transition was found to belong also to the level scheme of $^{130}$Sb populated from the decay of the $7^-$-state in $^{130}$Sn [13]. From [1] a $Q_\beta$-value of 5900(300) keV for the decay from the $(8^-)$-state was reported which is about 0.9 MeV above the value determined in our work.

In the discussion about the origin of this discrepancy one has to take into account, that the precision of β-decay energies obtained from $Q_\beta$-measurements firstly depends on the energy of the β-transition, since the higher the β-decay energy is, the higher the total number of events in the spectrum has to be. Secondly, it depends on the energy of the coincident γ-transition, since the lower the energy of the gate is, the more important the influence of electrons coincident to compton scattered γ-rays becomes. Furthermore, the latter effect depends on the endpoint energy of the β-transition. For example the background handling in the β-spectra coincident to 409 keV γ-ray following the decay of $^{130}$In was straight forward, since at energies above 6 MeV electrons coincident to scattered γ-rays did not contribute. Instead, in the case of the transitions following the decay of the negative parity state in $^{130}$Sb it was not possible to distinguish between contributions of electrons coincident to scattered γ-rays and a possible high energy component. Due to the weakness of these γ-transitions only

**Table 4.** Summary of experimental mass excesses $M_{exp}$ obtained for antimony, tin and indium isotopes with masses $A=128$ and 130 and comparisions with different mass formulae predictions $M_{pred}$

| Nuclide | $M_{exp}$ [MeV] | $M_{exp}-M_{pred}$ [MeV] | | | | | | | | |
|---|---|---|---|---|---|---|---|---|---|---|
| | | [14] | [15] | [16] | [17] | [18] | [19] | [20] | [21] | [22] |
| $^{128}Sb$ | −84.60 (0.03) | −0.48 | −0.44 | 0.21 | 0.19 | −0.06 | −0.04 | −0.57 | −0.11 | −0.41 |
| $^{128}Sn$ | −83.34 (0.03) | −0.14 | −0.03 | 0.06 | −0.08 | 0.06 | −0.54 | −0.32 | −0.05 | −0.01 |
| $^{128}In$ | −74.43 (0.10) | 0.15 | 0.08 | 0.50 | 0.28 | 0.13 | −0.08 | −0.12 | −0.02 | 0.01 |
| $^{130}Sb$ | −82.39 (0.03) | −0.46 | −0.41 | 0.06 | 0.11 | −0.03 | −0.50 | −0.28 | 0.15 | −0.35 |
| $^{130}Sn$ | −80.24 (0.03) | −0.05 | −0.05 | −0.26 | −0.35 | −0.18 | −0.78 | 0.01 | −0.14 | −0.11 |
| $^{130}In$ | −70.36 (0.10) | −0.04 | −0.03 | 0.78 | 0.59 | −0.05 | −0.29 | −0.20 | −0.18 | −0.06 |

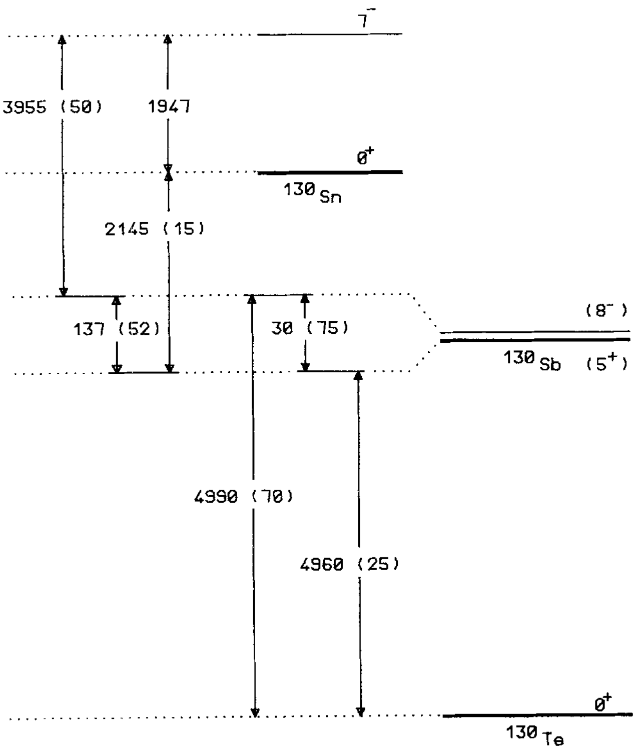


**Fig. 2.** Schematic summary of $\beta$-decaying states and decay energies of tin, antimony and tellurium nuclei with mass $A=130$

the branches with $E_\beta$-values which are shown in Table 2 could unambiguously be identified. It should be noted though that the $E_\beta$ value for $^{130}Sb(8^-)$ results from subtraction of an intense background component.

As consequence, the continuation of this discussion has to be based on further experimental data. On the other side it has become obvious, that to reinvestigate the decay of the negative parity state in $^{130}Sb$ not necessarily very strong sources have to be used, but that contributions from other $\beta$-decaying nuclei with high energy electrons have to be carefully suppressed.

## 6. Calculation of nuclear masses

Starting from that member of an isobaric chain, whose mass is known, the masses of isobars further away from the line of $\beta$-stability are determined by adding measured total $\beta$-decay energies. Based on the masses of the stable tellurium isotopes [14] in Table 4 the mass excesses of antimony, tin and indium isotopes with masses $A=128$ and 130 are compared with mass formulae predictions based on empirical models [15, 18, 20–22], the liquid drop model with shell corrections [16], the finite range droplet model [17] and the infinite nuclear matter model [19]. Although restricted to a limited number of experimental data the comparison allows to test mass formulae predictions for nuclei far away from the line of $\beta$-stability but also near a doubly closed-shell nucleus. To classify the individual models one finds from a comparison of the experimental and the calculated mass values of the different indium, tin and antimony nuclei that for both the $A=128$ and 130 nuclei a predictive quality better than 0.2 MeV is only achieved by four models. The models of Dussel et al. [15] and Masson et al. [22] reproduce the mass values of tin and indium nuclei with masses $A=128$ and 130 within this limit but fail in estimating the values for the antimony nuclei, whereas the models of Comay et al. [18] and Jänecke et al. [21] show an agreement for all 6 nuclei investigated. On the other side one has to take into account the character of the different models and that due to the inherent procedure of the empirical mass formulae the extrapolation by a few nucleons is always rather good.

For financial support of this work the authors are indebted to the Bundesministerium für Forschung und Technologie.

## References

1. Kerek, A., Carle, P., McDonald, J.: Nucl. Phys. A **198**, 466 (1972)
2. Lund, E., Aleklett, K., Rudstam, G.: Nucl. Phys. A **286**, 403 (1977)
3. Aleklett, K., Lund, E., Rudstam, G.: Phys. Rev. C **18**, 462 (1978)
4. Kerek, A., Holm, G.B., Borg, S., Carle, P.: Nucl. Phys. A **209**, 520 (1973)
5. Fogelberg, B., Aprahamian, A., Gill, R.L., Mach, H., Rehfield, D.: Phys. Rev. C **31**, 1026 (1985)
6. Hörner, St., Denschlag, H.O., Gabelmann, H., Kratz, K.L., Pfeiffer, B., Stöhlker, U.: NEANDC(E) – 262U Vol. V. INDC(GER)-28 LN + SPECIAL: 43–46 (1985)
7. Münzel, J., Wollnik, H., Pfeiffer, B., Jung, G.: Nucl. Instrum Methods **186**, 343 (1981)
8. Blönnigen, A., Bewersdorf, G., Geisse, Ch., Lippert, W., Pfeiffer, B., Stöhlker, U., Wollnik, H.: AMCO Conference 7 (1984) 134

9. Lippert, W.: Thesis; University of Giessen unpublished 1985
10. Fogelberg, B., Spanier, L.: Private communication 1986
11. Lewis, L., Nunnelley, L., Loveland, W.: Phys. Rev. C**13**, 2017 (1976)
12. Fogelberg, B., Heyde, K., Sau, J.: Nucl. Phys. A**352**, 157 (1981)
13. Stöhlker, U.: Ph.D. Thesis; University of Giessen: unpublished 1986
14. Wapstra, A.H., Audi, G., Hoekstra, R.: At. Data Nucl. Data Tables **39**, 281 (1988)
15. Dussel, G., Caurier, E., Zuker, A.P.: At. Data Nucl. Data Tables **39**, 205 (1988)
16. Möller, P., Nix, J.R.: At. Data Nucl. Data Tables **39**, 213 (1988)
17. Möller, P., Myers, W.D., Swiatecki, W.J., Treiner, J.: At. Data Nucl. Data Tables **39**, 225 (1988)
18. Comay, E., Kelson, I., Zidon, A.: At. Data Nucl. Data Tables **39**, 235 (1988)
19. Satpathy, L., Nayak, R.C.: At. Data Nucl. Data Tables **39**, 241 (1988)
20. Tachibana, T., Uno, M., Yamada, M., Yamada, S.: At. Data Nucl. Data Tables **39**, 251 (1988)
21. Jänecke, J., Masson, P.J.: At. Data Nucl. Data Tables **39**, 265 (1988)
22. Masson, P.J., Jänecke, J.: At. Data Nucl. Data Tables **39**, 273 (1988)

U. Stöhlker
Fuchshaldengässle 1
D-7801 Ebringen
Federal Republic of Germany

A. Blönnigen, W. Lippert, H. Wollnik
II. Physikalisches Institut
der Justus-Liebig-Universität Giessen
D-6300 Giessen
Federal Republic of Germany